Experimental and first-principles study of photoluminescent and optical properties of Na-doped $CuAlO_2$: the role of the $Na_{Al}$-$2Na_i$ complex



2015 J. Phys. D: Appl. Phys. 48 335102

(http://iopscience.iop.org/0022-3727/48/33/335102)

IOP Publishing Journal of Physics D: Applied Physics
J. Phys. D: Appl. Phys. **48** (2015) 335102 (6pp) doi:10.1088/0022-3727/48/33/335102

# Experimental and first-principles study of photoluminescent and optical properties of Na-doped $CuAlO_2$: the role of the $Na_{Al}$-$2Na_i$ complex

**Ruijian Liu[1], Yongfeng Li[1,2,5], Bin Yao[1,2,5], Zhanhui Ding[1], Rui Deng[3], Ligong Zhang[4], Haifeng Zhao[4] and Lei Liu[4]**

[1] State Key Lab of Superhard Material and Department of Physics, Jilin University, Changchun 130012, People's Republic of China
[2] Key Lab of Physics and Technology for Advanced Batteries, Ministry of Education and department of physics, Jilin University, Changchun 130012, People's Republic of China
[3] School of Materials Science and Engineering, Changchun University of Science and Technology, Changchun, 130022, People's Republic of China
[4] State Key Lab of Excited State Processes, Changchun Institute of Optics, Fine Mechanics and Physics, Chinese Academy of Sciences, Changchun, 130033, People's Republic of China

E-mail: liyongfeng@jlu.edu.cn and binyas@jlu.edu.cn

Received 11 March 2015, revised 12 June 2015
Accepted for publication 23 June 2015
Published 20 July 2015


**Abstract**

We report that a band-tail emission at 3.08 eV, lower than near-band-edge energy, is observed in photoluminescence measurements of bulk Na-doped $CuAlO_2$. The band-tail emission is attributed to Na-related defects. Electronic structure calculations based on the first-principles method demonstrate that the donor-acceptor compensated complex of $Na_{Al}$-$2Na_i$ in Na-doped $CuAlO_2$ plays a key role in leading to the band-tail emission and bandgap narrowing. Furthermore, Hall effect measurements indicates that the hole concentration in $CuAlO_2$ is independent on Na doping, which is well understood by the donor-acceptor compensation effect of $Na_{Al}$-$2Na_i$ complex.

Keywords: $CuAlO_2$, Na doping, photoluminescence, optical property, first-principles calculation

(Some figures may appear in colour only in the online journal)

## 1. Introduction

Transparent conducting oxides (TCO) are materials of electrical conduction with visible light transmission. Especially, their applications consist of flat panel displays, solar cells, liquid crystal displays, touch screen, and smart mobile phone [1]. Nowadays, the TCO materials are mainly used n-type semiconductors such as indium tin oxide (ITO) [2, 3], zinc oxide (ZnO) [4–6] and tin oxide ($SnO_2$) [7–9], which are commercially available, whereas the materials for p-type conductor of TCO are still being discovered. The lack of high quality and stable *p*-type TCO severely restricts the development of *p*–*n* junction based devices, such as laser diodes [10], transistors [11] and so on.

Delafossite oxides $ABO_2$ (A is Cu and Ag, B is trivalent cation, such as Al, Cr, Fe, Y, La, Sc) have been of great interest since it was reported by Kawazoe *et al* [12] that the delafossite $CuAlO_2$ thin film is a *p*-type TCO material due to the direct energy gap in 3.5 eV with positive Seebeck coefficient and the electrical conductivity can be upto 1 S cm$^{-1}$ at room temperature. Up to now, the conductivities of these *p*-type TCO materials are still much lower than those of *n*-type TCO materials. With the aim to enhance p-type conductivities, a plenty variety of experiments

[5] Authors to whom any correspondence should be addressed.

 

about isoelectronic doping on A-site [13, 14] or acceptor-doping on B-site [15–18] as well as nonstoichiometric (excess oxygen and/or excess metal cations) [10, 19, 20] in these delafossite oxides have been studied. However, among those experiments, the doping elements are commonly from group IIA, IB, IIB and VIIIB but seldom from group IA. The group IA elements substituted on A-site in $ABO_2$ play the role of isoelectronic doping, which can influence its electronic structure, optical and photoluminescent as well as electrical properties. Therefore, it is of significance to study isoelectronic doping in $CuAlO_2$ for improving p-type conduction and understanding doping mechanism.

In this paper, bulk Na-doped $CuAlO_2$ is synthesized by conventional direct solid-state reaction. The structural, electrical and optical properties of the Na-doped $CuAlO_2$ were systematically investigated. The physical mechanism of the effect of Na dopants on electronic structures, optical and electrical properties is also elucidated using first-principles calculations.

## 2. Experimental and first-principles calculations section

Bulk Na-doped $CuAlO_2$ was synthesized by a conventional direct solid-state reaction method. First, stoichiometric high-purity powders CuO (99.99%), $Al_2O_3$ (99.99%, 5 $\mu$m), and $Na_2CO_3$ ($\geqslant$99.95%) were sufficiently well mixed and ground in an agate mortar to ensure homogeneity. Na concentrations in the samples were controlled by mixing different amounts of $Na_2CO_3$. Then, a homogenous mixture was obtained and mechanically pressed into the disks with a diameter of 13 mm and a thickness of 1.5 mm. Finally, the disks were sintered in furnace at 1473 K under air atmosphere for 2 h. We obtained four samples, labeled as CAO, CAONa1, CAONa2 and CAONa3, corresponding to the Na concentration of 0, 7.04%, 7.20% and 8.91%, respectively.

The crystal structures of all samples were characterized by x-ray diffraction (XRD) using a Rigaku D/max-2550 x-ray diffractometer equipped with Cu Kα radiation ($\lambda$ = 1.5406 Å). The carrier concentration, mobility, resistivity, and conduction type of the samples were obtained from the Hall effect measurements in the Van der Pauw configuration at room temperature. The surface morphology was characterized by HITACHI S-4800 field-emission scanning electron microscopy (FE-SEM). The photoluminescence (PL) measurements were performed on a fluorescence spectrometer (Dongwoo MonoRa Instruments) at room temperature using He-Cd laser as the excitation source with a 325 nm line. The Raman spectra from the samples were collected at room temperature using a Horiba Jobin-Yvon T64000 Raman spectrometer equipped with 532 nm excitation lasers. To determine Na concentration in the samples, x-ray photoelectron spectroscopy (XPS) was performed using an ESCALAB 250 XPS instrument with Al Kα ($h\nu$ = 1486.6 eV) x-ray radiation source, which can precisely calibrate work function and Fermi energy level. All XPS spectra were calibrated by the C 1 s peak (284.6 eV).

In order to make it clear what defects caused the emission at 3.08 eV (seen in figure 2), a model of $CuAlO_2$ doped with $Na_{Al}$-2$Na_i$ complex was proposed and calculated using a first-principles method. The calculations were carried out using the VASP code with the projector augmented wave (PAW) potentials and the general gradient approximation (GGA) was taken to obtain a relatively reasonable result. The cutoff energy for the plane-wave basis set is 400 eV. Since our experimental findings did not give any indication of the intrinsic defect related photoluminescence, we have not created any intrinsic defects deliberately in the calculations. A 108 atom 3 × 3 × 1 $CuAlO_2$ supercell was constructed with the delafossite structure as a reference and four types of Na related defects were considered: (i) interstitial Na ($Na_i$), created by adding a Na atom at the interstitial site inside the supercell, (ii) Na substituting Cu ($Na_{Cu}$) and (iii) Na substituting Al ($Na_{Al}$), created by replacing a Cu and Al atom with a Na atom, respectively, (iv) $Na_{Al}$-2$Na_i$ complex, built by replacing an Al atom with a Na atom and inserting two extra Na atoms into the supercell adjacent to $Na_{Al}$. In all calculations, all the atoms are allowed to relax until the Hellmann − Feynman forces acting on them become less than 0.01 eV Å$^{-1}$ and self-consistency was achieved with a tolerance in total energy of $10^{-4}$ eV. The optimized a- and *c*-axis lattice parameters of perfect $CuAlO_2$ are 2.849 Å and 17.037 Å with a small error of 0.3% and 0.5% with respect to experimental values ($a$ = 2.858 Å, $c$ = 16.958 Å) reported in literature for $CuAlO_2$ [21] and which is, respectively, in good agreement with the corresponding experimental values ($a$ = 2.857 Å, $c$ = 16.941 Å) obtained in the present study, indicating that our calculation is reasonable and reliable.

## 3. Results and discussion

### 3.1. Component, crystal structure and surface morphology

The XRD patterns of all $CuAlO_2$ samples are shown in figure 1(a). The reference powder diffraction data (PDF 77–2493) is also presented as a contrast. For the samples CAO and CAONa1, only the diffraction peaks of delafossite $CuAlO_2$ are observed and no secondary phase is observed. For the samples CAONa2 and CAONa3, besides diffraction peaks of $CuAlO_2$, the weak diffraction peaks of CuO phase are also observed, indicating that there is a slight amount of CuO in the samples. No Na-related phases are observed for all samples.

To further study the doping effect on the structure caused by the Na-related defects, Raman scattering spectra of all $CuAlO_2$ samples were carried out, as shown in figure 1(b). There are two typical vibrational bands at 417 cm$^{-1}$ and 766 cm$^{-1}$ for all samples, which is ascribed to $E_g$ and $A_{1g}$ modes of delafossite $CuAlO_2$, respectively. The *A* modes imply movement in the direction of Cu-O bonds, whereas double degenerate *E* modes describe vibration in the perpendicular direction [22]. In addition, four weak Raman features with shifts around 227 cm$^{-1}$, 259 cm$^{-1}$, 607 cm$^{-1}$ and 656 cm$^{-1}$ are also observed and labeled in figure 1(b). Pellicer-Porres *et al* reported the four featured peaks also originates from $CuAlO_2$ [22], It should be noted that, for the samples CAONa2 and CAONa3, there are two weak peaks centered at 292 cm$^{-1}$ and 341 cm$^{-1}$, respectively, corresponding to the $A_g$ and $B_g$ modes of CuO

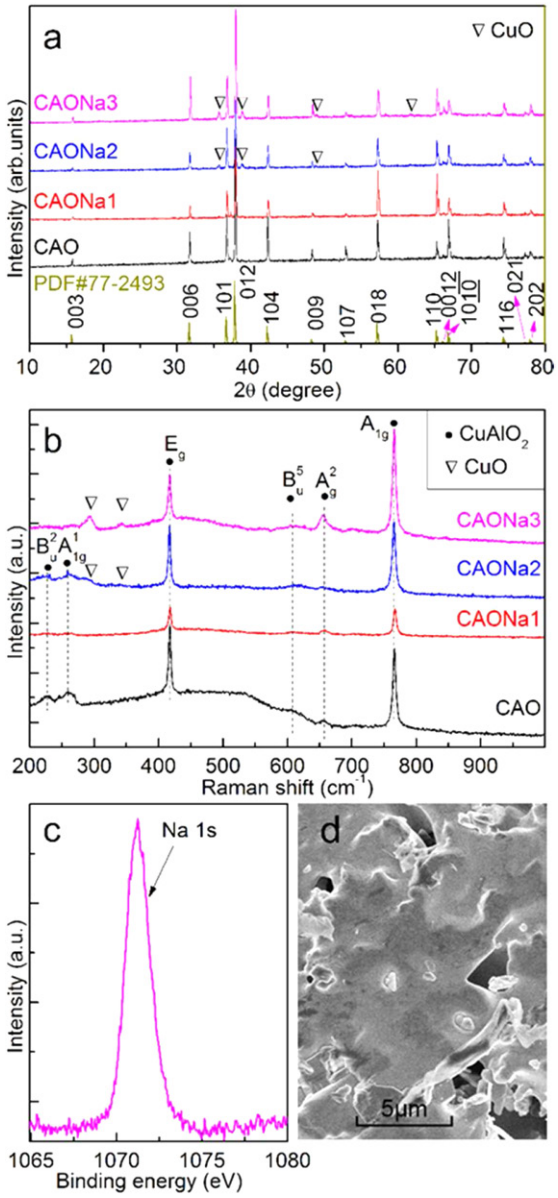


**Figure 1.** Structural, componential characterizations and surface morphology of Na-doped $CuAlO_2$. (a) XRD patterns and (b) Raman spectra of all $CuAlO_2$ samples. The reference powder diffraction data (PDF 77–2493) is also presented in (a). The typical (c) Na 1 s XPS spectroscopy and (d) SEM photograph of the Na-doped $CuAlO_2$ with a Na concentration of 8.91%.

phase [23], suggesting the existence of CuO phase in $CuAlO_2$ and in agreement with XRD results.

Figure 1(c) shows a typical Na 1s XPS spectroscopy of the Na-doped $CuAlO_2$ with Na concentration of 8.91% (CAONa3). The peak of Na 1s at 1071.2 eV, indicating that the chemical valence of Na is +1 in $CuAlO_2$ [24]. A typical surface morphology of the Na-doped $CuAlO_2$ (CAONa3) is shown in figure 1(d).

### 3.2. Photoluminescence

Figure 2 shows room temperature PL spectra of all samples. A strong UV emission peak at 368 nm (3.37 eV) is observed for the pure $CuAlO_2$, which is attributed to the near-band-edge

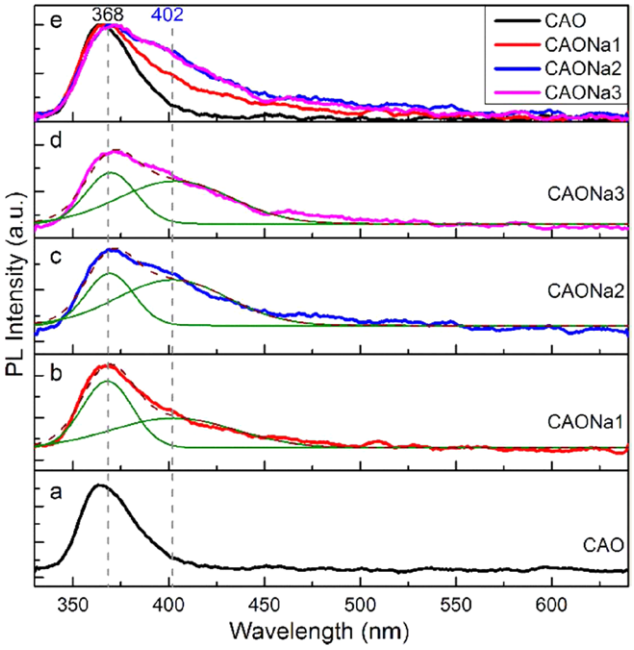


**Figure 2.** (a)–(d) Room temperature PL spectra of all $CuAlO_2$ samples with various Na concentrations and (e) the corresponding normalized PL spectra.

(NBE) emission of $CuAlO_2$ [25]. Interestingly, a distinct emission shoulder centered at 402 nm (3.08 eV) is observed for all Na-doped $CuAlO_2$. To clearly see the shoulder, the fitting Gaussian curves to the PL spectra of Na-doped $CuAlO_2$ are shown in figures 2(b)–(d) and the corresponding normalized PL spectra are shown in figure 2(e). Obviously, the shoulders at 3.08 eV, as a band-tail emission, are derived from the Na-related defects. The defect level related to Na dopants is estimated to be 0.29 eV.

### 3.3. Electrical properties

To check the effect of Na doping on electrical properties of $CuAlO_2$, we performed Hall effect measurements for all samples. The measured results are listed in table 1. It is found that all the samples show *p*-type conductivity with an almost the same hole concentration of ~$10^{17}$ $cm^{-3}$. These results suggest that, although the photoluminescence of Na-doped $CuAlO_2$ can be modified by Na doping, the electrical properties is independent on Na doping.

### 3.4. First-principles calculations of electronic structure and optical properties

To investigate the effect Na doping on optical properties of $CuAlO_2$, electronic structure of Na-doped $CuAlO_2$ was calculated by the first-principles methods. We first checked the band structures of the $CuAlO_2$ with several typical Na-related defects, as shown in figure 3. The highest occupied state is set at zero in these band structures. For the perfect $CuAlO_2$, the conduction-band minimum (CBM) and valence-band maximum (VBM) are not at the same point of reciprocal space, indicating an indirect bandgap, in good agreement with the

**Table 1.** The electrical properties of the bulk CAONa samples.

| Na concentration | Resistivity (Ω cm) | Carrier density ($cm^{-3}$) | Mobility ($cm^2V^{-1}s^{-1}$) | Conduction type |
|---|---|---|---|---|
| 0 | 76.3 | $3.8 \times 10^{17}$ | $2.2 \times 10^{-1}$ | p |
| 7.04% | 76.6 | $5.7 \times 10^{17}$ | $1.4 \times 10^{-1}$ | p |
| 7.20% | 74.2 | $2.2 \times 10^{17}$ | $3.8 \times 10^{-1}$ | p |
| 8.91% | 90.3 | $1.7 \times 10^{17}$ | $4.0 \times 10^{-1}$ | P |

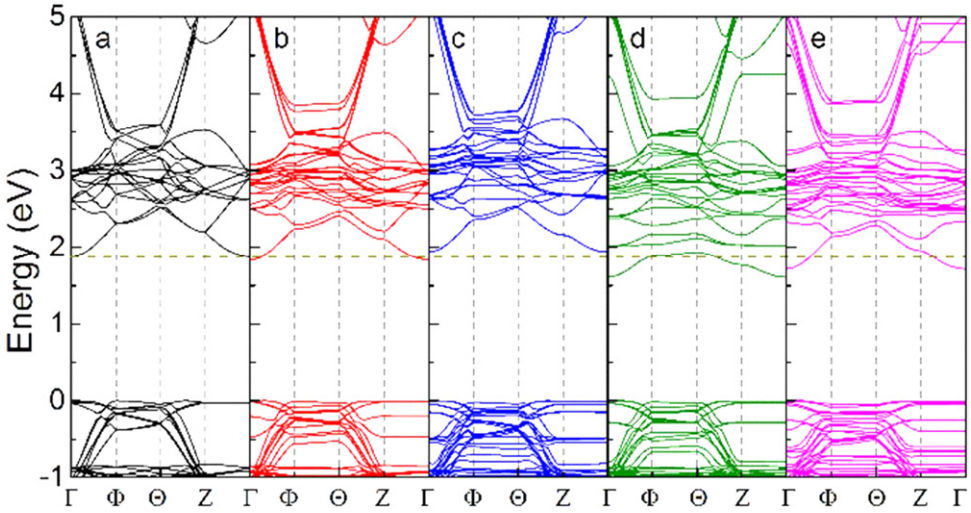


**Figure 3.** Band structures of the $CuAlO_2$ supercells (a) without and with (b) $Na_{Cu}$, (c) $Na_{Al}$ (d) $Na_i$ and (e) $Na_{Al}$-$2Na_i$ complex. The highest occupied state is set at zero.

results from previous reports [26, 27]. the value of the direct bandgap at Γ is 1.91 eV, smaller than the experimental value of ~3.5 eV [12] due to the well-known underestimation of bandgap using GGA method, but it does not affect our discussion on the results. For the $Na_{Cu}$, as an isoelectronic dopant, no defect state is found and the bandgap shows a very slight narrowing of 0.06 eV with respect to perfect $CuAlO_2$, which is much smaller than 0.29 eV from the PL spectra. It is not consistent with experimental results. For the $Na_{Al}$, as an acceptor, it is found that the bandgap is slight wider than perfect $CuAlO_2$, which is not in agreement with the experimental result. For the $Na_i$, as a donor, a significant bandgap narrowing is obtained. However, if there exists a large amount of isolated $Na_i$, the hole concentration will significantly decreases due to the compensation of donor to acceptor. Therefore, the band-tail emission is not derived from the isolated $Na_i$. Interestingly, we find that the donor-acceptor complex of $Na_{Al}$-$2Na_i$ induces a fully compensated band above the VBM and leads to a significant decrease of 'effective' bandgap (difference between CBM to the top of the fully occupied compensation band). Differing from the indirect bandgap of the perfect $CuAlO_2$, the 'effective' bandgap of $CuAlO_2$ with $Na_{Al}$-$2Na_i$ complex is a direct one at Γ with a value of 1.71 eV. It should be noted that narrow of 0.2 eV with respect to perfect $CuAlO_2$ is near the value from the PL result. In addition, the $Na_{Al}$-$2Na_i$ complex is not able to modify the hole concentration because it does not contribute carriers to conduction- or valence-band and not compensate carriers.

We further calculated the optical absorption spectra of Na-doped $CuAlO_2$. Figure 4(a) shows the polarized optical absorption spectra of $CuAlO_2$ with and without Na-related

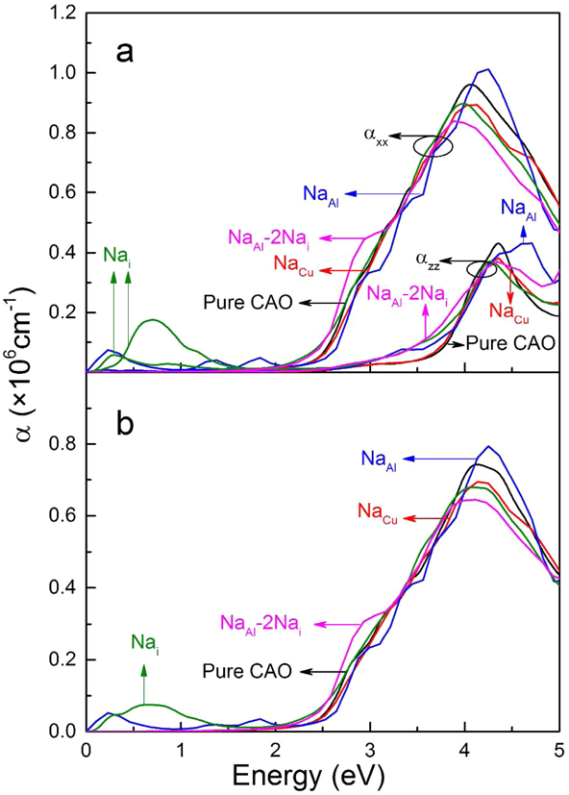


**Figure 4.** Calculated (a) polarized and (b) polycrystalline optical absorption spectra of the $CuAlO_2$ supercells with different Na-related defects.

defects. To simulate the optical properties of the polycrystalline $CuAlO_2$, the polarized absorption from *x*-, *y*- and *z*-direction is

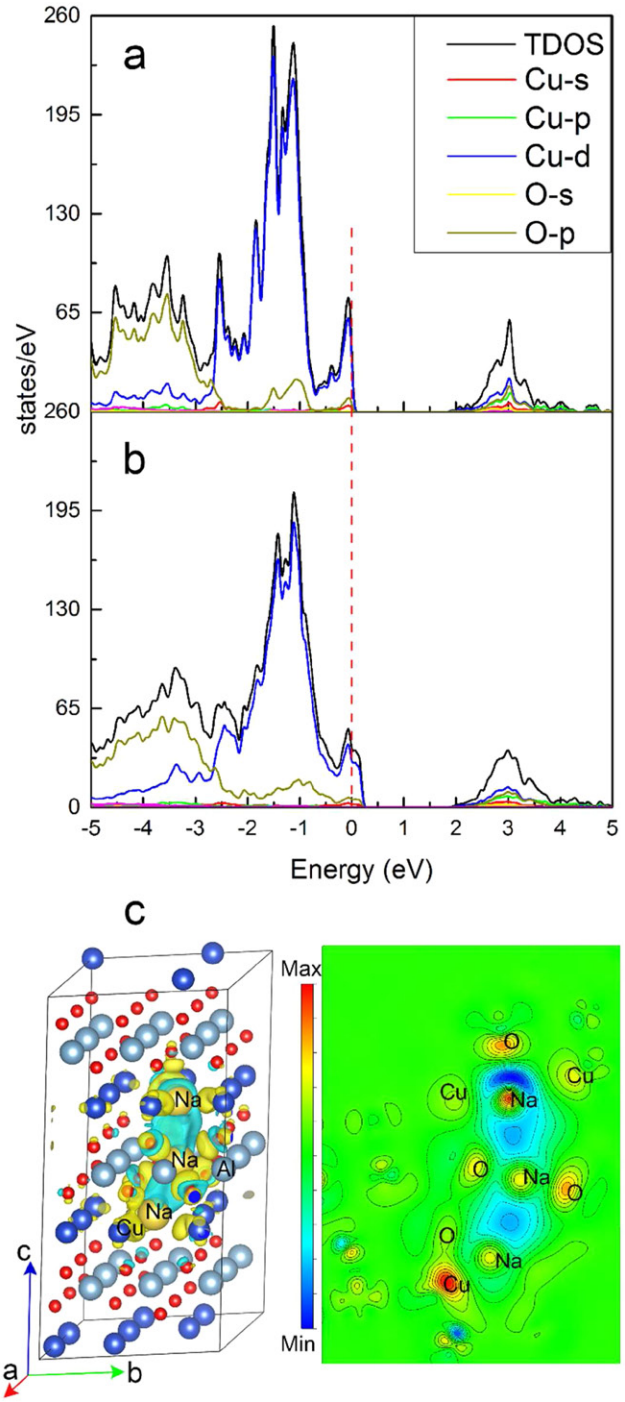


**Figure 5.** Total and partial DOS of the $CuAlO_2$ supercells (a) without and (b) with $Na_{Al}$-$2Na_i$ complex. (c) Differential charge density of $CuAlO_2$ supercell with $Na_{Al}$-$2Na_i$ complex in the supercell (left) and its contour map on the co-plane of three Na atoms (right).

averaged, as shown in figure 4(b). Only the absorption edge for the $CuAlO_2$ with a $Na_{Al}$-$2Na_i$ complex has a significant red-shift with 0.2 eV, consistent with the calculated band structure. For the $CuAlO_2$ with $Na_{Cu}$ and $Na_{Al}$ defects, the absorption edges don't nearly shift with respect to the perfect $CuAlO_2$. These calculated results suggest that the $Na_{Al}$-$2Na_i$ complex in $CuAlO_2$ is the derivation of the band-tail emission at 3.08 eV in the PL spectra of Na-doped $CuAlO_2$.

To well understand the effect of compensated $Na_{Al}$-$2Na_i$ complex on optical absorption spectra of $CuAlO_2$, the total and partial density of state (DOS) of $CuAlO_2$ without and with $Na_{Al}$-$2Na_i$ complex is also calculated, as shown in figures 5(a) and (b), respectively. The VBM of the $CuAlO_2$ without $Na_{Al}$-$2Na_i$ complex is set as zero reference. Comparing with the perfect $CuAlO_2$, the $Na_{Al}$-$2Na_i$ complex generates an additional fully occupied band above the VBM, resulting in a significant narrowing of energy gap. The electron transition will occur between CBM and the $Na_{Al}$-$2Na_i$ occupied band as the photon with suitable energy is absorbed or emitted.

We finally checked the stability of the $Na_{Al}$-$2Na_i$ complex in $CuAlO_2$. The binding energy of $Na_{Al}$-$2Na_i$ complex in $CuAlO_2$ can be expressed as

$$E_b = E_{tot}(Na_{Al} - 2Na_i) + 2E_{tot}(CuAlO_2) - E_{tot}(Na_{Al}) - 2E_{tot}(Na_i) \quad (1)$$

where $E_{tot}$ is the total energies of the system calculated with the same supercell [8, 28–30]. A negative $E_b$ indicates that the complex tends to bind to each other when both are present in the sample. The calculated binding energy $E_b$ for the $Na_{Al}$-$2Na_i$ complex is −1.07 eV, indicating that the complex is stable with respect to the isolated $Na_{Al}$ and $Na_i$ defect. Furthermore, the differential charge density of $CuAlO_2$ with $Na_{Al}$-$2Na_i$ complex is shown in figure 5(c). These results help us to understand the stability of $Na_{Al}$-$2Na_i$ complex in $CuAlO_2$.

Finally, it is worth noting that, although the Na-doping in $CuAlO_2$ is unable to increase the conductivity due to the compensation effect of $Na_{Al}$-$2Na_i$ complex, the complex leads to an occupied bands above the VBM, equivalently pushing the VBM to higher energy. If we choose another acceptor element to co-dope to $CuAlO_2$ with Na doping, it is expected that the acceptor ionization is lower due to the occupied bands with higher energy.

## 4. Conclusions

We experimentally found a Na-related band-tail emission at 3.08 eV, lower than NBE energy, in the PL spectra of Na-doped $CuAlO_2$. The hole concentration is independent on Na doping. Theoretically, we investigated several typical Na-related defects in $CuAlO_2$ based on electronic structure calculations. A stable donor-acceptor compensated $Na_{Al}$-$2Na_i$ complex in $CuAlO_2$ results in the bandgap narrowing and the band-tail emission observed in PL spectra.

## Acknowledgments

This work is supported by the National Natural Science Foundation of China under Grant Nos. 10874178, 11074093, 61205038 and 11274135, Specialized Research Fund for the Doctoral Program of Higher Education under Grant No. 20130061130011, Ph.D. Programs Foundation of Ministry of Education of China under Grant No. 20120061120011, Natural Science Foundation of Jilin province under grant

No. 201115013, and National Found for Fostering Talents of Basic Science under grant No. J1103202.This work was also supported by High Performance Computing Center of Jilin University, China.

## References

[1] Ruttanapun C, Boonchom B, Thongkam M, Kongtaweelert S, Thanachayanont C and Wichainchai A 2013 *J. Appl. Phys.* **113** 023103
[2] Jeong S H, Lee S B and Boo J H 2004 *Curr. Appl. Phys.* **4** 655
[3] Gao J, Lebedev O I, Turner S, Li Y F, Lu Y H, Feng Y P, Boullay P, Prellier W, van Tendeloo G and Wu T 2012 *Nano Lett.* **12** 275
[4] Ramamoorthy K, Sanjeeviraja C, Jayachandran M, Sankaranarayanan K, Misra P and Kukreja L M 2006 *Curr. Appl. Phys.* **6** 103
[5] Jung S M, Kim Y H, Kim S I and Yoo S I 2011 *Curr. Appl. Phys.* **11** S191
[6] Li Y F, Deng R, Lin W N, Tian Y F, Peng H Y, Yi J B, Yao B and Wu T 2013 *Phys. Rev.* B **87** 155151
[7] Chenari H M, Golzan M M, Sedghi H, Hassanzadeh A and Talebian M 2011 *Curr. Appl. Phys.* **11** 1071
[8] Li Y F, Deng R, Tian Y F, Yao B and Wu T 2012 *Appl. Phys. Lett.* **100** 172402
[9] Li Y, Yin W, Deng R, Chen R, Chen J, Yan Q, Yao B, Sun H, Wei S-H and Wu T 2012 *NPG Asia Mater.* **4** e30
[10] Cai J L and Gong H 2005 *J. Appl. Phys.* **98** 033707
[11] Nomura K, Ohta H, Ueda K, Kamiya T, Hirano M and Hosono H 2003 *Science* **300** 1269
[12] Kawazoe H and Yasukawa M 1997 *Nature* **389** 939
[13] Yanagiya S-I, Ngo Van N, Xu J and Pryds N 2010 *Materials* **3** 318
[14] Ruttanapun C, Prachamon W and Wichainchai A 2012 *Curr. Appl. Phys.* **12** 166
[15] Dong G, Zhang M, Lan W, Dong P and Yan H 2008 *Vacuum* **82** 1321
[16] Dong P, Zhang M, Dong G, Zhao X and Yan H 2008 *J. Electrochem. Soc.* **155** H319
[17] Jiang H F, Wang X C, Zang X P, Wu W F, Sun S P, Xiong C, Yin W W, Gui C Y and Zhu X B 2013 *J. Alloys Compd.* **553** 245
[18] Pan J Q, Guo S K, Zhang X, Feng B X and Lan W 2013 *Mater. Lett.* **96** 31
[19] Banerjee A N, Ghosh C K and Chattopadhyay K K 2005 *Sol. Energy Mater. Sol. Cells* **89** 75
[20] Zhang Y J, Liu Z T, Feng L P and Zang D Y 2012 *Appl. Surf. Sci.* **258** 5354
[21] Nie X, Wei S H and Zhang S B 2002 *Phys. Rev. Lett.* **88** 066405
[22] Pellicer-Porres J, Martinez-Garcia D, Segura A, Rodriguez-Hernandez P, Munoz A, Chervin J C, Garro N and Kim D 2006 *Phys. Rev.* B **74** 184301
[23] Hagemann H, Bill H, Sadowski W, Walker E and François M 1990 *Solid State Commun.* **73** 447
[24] Nefedov V I, Salyn Y V, Leonhardt G and Scheibe R 1977 *J. Electron Spectrosc. Relat. Phenom.* **10** 121
[25] Banerjee A N and Chattopadhyay K K 2005 *J. Appl. Phys.* **97** 084308
[26] Huda M N, Yan Y F, Walsh A, Wei S H and Al-Jassim M M 2009 *Phys. Rev.* B **80** 035205
[27] Huang D and Pan Y M 2010 *Can. J. Phys.* **88** 927
[28] Gai Y Q, Tang G and Li J B 2011 *J. Phys. Chem. Solids* **72** 725
[29] Li J, Wei S H, Li S S and Xia J B 2006 *Phys. Rev.* B **74** 081201(R)
[30] Zhou H, Deng R, Li Y-F, Yao B, Ding Z-H, Wang Q-X, Han Y, Wu T and Liu L 2014 *J. Phys. Chem.* C **118** 6365